Antidepressants act by binding to the transmembrane domain of TRKB receptor

Authors:
Plinio C Casarotto[1], Mykhailo Girych[2], Senem M Fred[1], Rafael Moliner[1], Giray Enkavi[2], Caroline Biojone[1], Cecilia Cannarozzo[1], Cecilia A Brunello[1], Anna Steinzeig[1], Frederike Winkel[1], Sudarshan Patil[3], Stefan Vestring[4], Tsvetan Serchov[5], Vera Kovaleva[6], Cassiano RAF Diniz[1,7], Liina Laukkanen[1], Iseline Cardon[8], Hanna Antila[1,9], Tomasz Rog[2], Mart Saarma[6], Clive R Bramham[3], Claus Normann[4], Sari E Lauri[1,10], Ilpo Vattulainen[2,11], Eero Castrén[1]*

1. Neuroscience Center - HILIFE, University of Helsinki, Finland.
2. Department of Physics, University of Helsinki, Finland.
3. Department of Biomedicine and KG Jebsen Center for Research on Neuropsychiatric Disorders, University of Bergen, Norway.
4. Center for Neuromodulation, Department of Psychiatry and Psychotherapy, Medical Center, Faculty of Medicine, University of Freiburg, Germany.
5. Department of Stereotactic and Functional Neurosurgery, Laboratory of Stereotaxy and Interventional Neuroscience, Medical Center – University of Freiburg, Faculty of Medicine, University of Freiburg, Germany.
6. Institute of Biotechnology - HILIFE, University of Helsinki, Finland.
7. Department of Pharmacology. Ribeirão Preto Medical School. University of São Paulo, Brazil.
8. Brain Master Program, Faculty of Science, Aix-Marseille Université, Marseille, France.
9. Department of Neuroscience, Perelman School of Medicine, University of Pennsylvania, PA, USA.
10. Molecular and Integrative Biosciences Research Program, University of Helsinki, Finland.
11. Computational Physics Laboratory, Tampere University, Finland.

* corresponding author:
Eero Castren. eero.castren@helsinki.fi

Abstract

It is unclear how binding of antidepressant drugs to their targets gives rise to the clinical antidepressant effect. We have found that both typical and fast-acting antidepressants bind to a cholesterol interaction motif in the brain-derived neurotrophic factor (BDNF) receptor (tropomyosin-related kinase B - TRKB), a known mediator of neuronal plasticity and antidepressant responses [1–4]. Antidepressants bind to a cross-shaped configuration of dimerized TRKB transmembrane domains and facilitate synaptic localization and activation of TRKB by BDNF. Mutation of the TRKB cholesterol interaction site or cholesterol depletion impaired BDNF-mediated plasticity as well as cellular and behavioral responses to antidepressants *in vitro* and *in vivo*. We suggest that binding to and facilitation of BDNF signaling through TRKB is the common mechanism for antidepressant action, which proposes a framework for how molecular effects of antidepressants are translated into clinical mood recovery.

Introduction

Several targets for antidepressant drug action have been identified but it is not clear how binding to these targets are translated into the clinical effects. Classical antidepressants increase the synaptic levels of serotonin and noradrenaline by inhibition of reuptake or metabolism, while the rapid antidepressant effect of ketamine is attributed to inhibition of NMDA receptors [5,6]. However, the low affinity of 2R,6R-hydroxynorketamine (R,R-HNK), a ketamine metabolite with antidepressant-like activity, to NMDA receptors has called this mechanism into question [7,8]. Therefore, it is not clear whether there is a common mechanism behind the antidepressant effect.

Essentially all antidepressants, including ketamine and R,R-HNK, increase the expression of brain-derived neurotrophic factor (BDNF) and activate BDNF signaling through Neurotrophin Tyrosine Kinase Receptor 2 (TRKB) [2–4], but this effect has been considered to be indirect through the inhibition of serotonin transporter (5HTT) and NMDA receptors. BDNF mimics the effects of antidepressants in rodents while inhibiting TRKB signaling prevents these effects [2–4,9]. BDNF signaling through TRKB is a critical mediator of activity-dependent synaptic plasticity [1] and the antidepressant-induced BDNF-TRKB signaling reactivates a juvenile-like state of plasticity in the adult brain, which has been suggested to underlie the effects of antidepressant treatments on mood [4,10,11].

BDNF signaling is bidirectionally linked to brain cholesterol metabolism. BDNF, acting through TRKB, promotes production of cholesterol in neurons [12,13] and cholesterol regulates TRKB signaling [14]. Cholesterol is essential for neuronal maturation and proper synaptic transmission [15]. Since cholesterol does not pass the blood-brain barrier, neurons are dependent on locally synthesized cholesterol, mostly by astrocytes [16]. Synaptic cholesterol levels are low during the embryonic and early postnatal life but strongly increase during the 3rd postnatal week in mice [17], coinciding with the increase in BDNF expression and appearance of antidepressants effects on TRKB [4,18]. Many antidepressants interact with phospholipids and accumulate in cholesterol-rich membrane microdomains, such as lipid rafts [19]. These data prompted us to investigate the potential interactions between TRKB, cholesterol and antidepressants.

CARC motif regulates TRKB activation

Bioinformatic mining revealed a region in the TRKB transmembrane (TM) region that fulfils the criteria for inverted cholesterol recognition and alignment consensus motif (CARC) [20]. This motif is specific to TRKB and is not present in other TRK receptors (Fig. S1A). In primary cortical neurons, cholesterol at 20μM enhanced the effects of BDNF (10 ng/ml) on TRKB phosphorylation (pTRKB), but at higher concentrations (50-100 μM), cholesterol suppressed the effects of BDNF (Fig. 1A). Cholesterol promotes TRKB:PLC-γ1 interaction and TRKB surface exposure (Fig. S1B-F). The effects of BDNF on TRKB-PLC-γ1 interaction (Fig. 1E), as well as neurite branching (Fig. S1H), were prevented by prior treatment with pravastatin (1 μM/3d), an inhibitor of cholesterol synthesis [14]. A higher concentration of pravastatin (2 μM/5d) reduced survival of cultured cortical neurons and this effect was attenuated by exogenous cholesterol (20 μM), but not by BDNF (Fig. S1M,N), indicating that the effects of pravastatin are mediated through inhibition of cholesterol synthesis.

Mutation of the critical tyrosine 433 in the CARC domain [21] into phenylalanine (TRKB.Y433F) did not influence the binding affinity of BDNF (TRKB.wt= 0.081ng/ml; TRKB.Y433F= 0.076ng/ml; Fig. S4H). However, this mutation did reduce pTRKB at the PLC-γ1 interaction site Y816, but not at Y515 in fibroblasts (Fig. 1F, S1G). Protein complementation assay in neuroblastoma cells indicated that the Y433F mutation compromised BDNF-induced dimerization of TRKB, TRKB interaction with raft-restricted FYN (Fig. 1G,H), as well as TRKB translocation to lipid rafts (Fig. S3I).

Atomistic simulation of dimerization of TRKB TM helices disclosed five possible structures, but only the conformation where TM domains cross each other at the A443-G439 motif was stable in phosphatidylcholine bilayer with 20-40 mol% cholesterol (Fig. 1B,C). The Y433 residue stabilizes the structure, and Y433F mutation destabilized it by rotating the TM monomers 40 degrees relative to each other (Fig. 1D). Modeling (Table S1) suggests that the increase in membrane thickness by cholesterol regulates the TM dimer structure (Fig. S2A), although cholesterol binding to the CARC motif is transient (residence times ~100ns or less). In the absence of cholesterol, the distance between the TRKB TM C-termini was about 2.2

nm, but at 40 mol% cholesterol, the dimer structure switched from the stable cross-like structure seen at 20 mol% to a more parallel conformation (distance ~1.5 nm, Fig. 1C, S2B). This is consistent with our experimental data suggesting an optimal cholesterol concentration for TRKB function. TRKB function was compromised at low cholesterol concentrations, where the large distance between the C-termini (Fig. S2) likely disrupts the conformation of the TRKB ectodomain [22], and also at high concentrations, where the more parallel orientation of cross-shaped structure is presumably unstable (Fig. 1C).

Antidepressants bind to TRKB CARC domain

Antidepressants are known to interact with phospholipids and accumulate to lipid rafts [19]. We found that several antidepressants mimicked the effects of cholesterol and enhanced TRKB:PLC-γ1, and PLC-γ1:pTRKB.Y816 interaction in primary cortical neurons, and this effect was blocked by the cholesterol-sequestering agent β-cyclodextrin (βCDX) (Fig. S3A-H). Furthermore, fluoxetine increased the surface expression of TRKB in cortical neurons, and this effect was also prevented by βCDX (Fig. S3F). These data suggest that antidepressants might interact with the TRKB cholesterol binding site.

We then assayed for the binding of antidepressants to TRKB. We found that biotinylated fluoxetine and R,R-HNK, as well as tritiated imipramine, all bind to immunoprecipitated TRKB with a low μM affinity (Kd= 2.42, 1.43, and 1.82μM, respectively; Fig. 2A,B, S4A). Although imipramine and fluoxetine bind to serotonin transporter (5HTT) with an affinity orders of magnitude higher than that for TRKB, micromolar affinity corresponds well to the concentrations reached in the human brain during chronic treatment [24,25]. The same compounds showed significantly lower affinity when assayed with TRKB.Y433F(Fig. 2A,B S4A), confirming binding to the CARC site. Ketamine, esketamine, R,R-HNK and imipramine displaced labeled fluoxetine (1 μM) binding with variable efficacy (Fig. S4C-E). However, BDNF failed to displace fluoxetine from TRKB (Fig. S4F), and negative control compounds 2S,6S-HNK, isoproterenol, chlorpromazine and diphenhydramine produced weak, if any displacement (Fig. S4G,H). We confirmed the direct interaction between fluoxetine and GFP-tagged TRKB using microscale thermophoresis assay (MST) [23] in HEK293T cell lysates (Fig. 2C). Together these results suggest that all of the investigated antidepressants interact with the TRKB CARC motif at clinically meaningful concentrations [24]. Furthermore, they identify TRKB as the so far elusive direct target for R,R-HNK [7,8].

Next, we used molecular dynamics to simulate the binding of fluoxetine to the TRKB TM structure. Docking of neutral fluoxetine to each of the four crevices created by the cross-shaped TRKB dimers using 30 different protein conformations (1 μs-long molecular dynamics sampling in a 20 mol% cholesterol membrane) revealed a binding site for fluoxetine in the crevice facing the extracellular side (Fig. 2D). Repositioning the drug around the binding pocket in 120 molecular dynamics simulations revealed a long-lasting stable association that overlapped with the CARC motif and was further stabilized by phospholipids (Fig. S5), confirming that fluoxetine directly binds to TRKB TM dimers. Twenty independent simulations starting from an equilibrated stable protein-fluoxetine complex showed that the Y433F mutation significantly reduced the residence-time of fluoxetine in TRKB homodimers (161ns and >696ns for the mutant and wild-type forms, respectively), indicating that the mutant protein cannot form a stable binding pocket.

When simulated at 40 mol% of cholesterol, fluoxetine promoted the retention of TRKB dimers in the active state that is close to the one observed in 20 mol% cholesterol, maintaining the separation between the C-termini, which is consistent with our biochemical observations (Fig. 1A). Following drug expulsion, the simulations invariably transitioned to the more parallel conformation seen in Fig. 1C. These data suggest that fluoxetine binding to the dimeric TRKB interface acts as a wedge, stabilizing the cross-shaped active conformation at high cholesterol concentration typically present in the synaptic membrane.

TRKB CARC motif modulates plasticity

We evaluated the mobility of GFP-tagged TRKB in neuronal spines using fluorescence recovery after photobleaching (FRAP) assay in transfected hippocampal primary cultures (DIV14). TRKB fluorescence is rapidly recovered in neurite shafts after bleaching (Fig. S6A), however no recovery was seen in spines (Fig. 3A-D). Treatment of neurons with fluoxetine, ketamine or BDNF promoted fluorescence recovery of

GFP-TRKB in spines within two minutes, but no facilitation was seen in cells transfected with GFP-tagged TRKB.Y433F (Fig. 3E-J). Furthermore, both BDNF and fluoxetine increased the size of TRKB clusters at the plasma membrane in fibroblasts, as measured by dSTORM/TIRF superresolution microscopy, and these effects were attenuated in cells expressing TRKB.Y433F (Fig. 3O). Thus, BDNF [14] or antidepressant [26] induced TRKB translocation to the plasma membrane and clustering are dependent on the TRKB CARC domain (Fig. 3, S3I). However, the TRKB.Y433F mutation does not change the basal surface localization of TRKB (Fig. 3O).

Infusion of BDNF into the dentate gyrus of anesthetized rats significantly increased synaptic strength, as previously reported [27]. However, this effect of BDNF was partially prevented when rats were co-treated with pravastatin (10 mg/kg/day for two weeks; Fig. 4A). To investigate whether this effect of BDNF on LTP involves the TRKB CARC motif, we generated a mouse carrying the TRKB.Y433F mutation. Theta-burst stimulation of hippocampal slices from wild-type mice induced a robust LTP in the CA3-CA1 synapse. Remarkably, similar stimulation of slices from heterozygous TRKB.Y433F mice failed to induce any potentiation (Fig. 4B), indicating that TRKB CARC motif is critical for LTP. However, tetanic stimulation induced LTP in both WT and TRKB.Y433F slices (Fig. S5C,E), consistent with the central role of BDNF role particularly in theta-burst mediated LTP [28].

Fluoxetine (15mg/kg, 7 days) improved performance of mice in object location memory (OLM) test. The improved performance by fluoxetine was blocked in heterozygous TRKB.Y433F (Fig. 4C) and in BDNF haploinsufficient mice (Fig. S6E). Remarkably, the serotonin transporter knockout (5HTT.ko) mice lacking the primary site of action of SSRIs respond to fluoxetine normally in the OLM test (Fig. S6F). This is consistent with the recent finding that the behavioral and electrophysiological effects of SSRIs are preserved in 5HTT.ko mice [29] (however, see [30]).

Ketamine (10mg/kg single i.p. injection) and fluoxetine (15mg/kg in the drinking water, for 3 weeks) reduced immobility in the forced-swimming test, but they were ineffective in TRKB.Y433F mice (Fig. 4E,F). Furthermore, fluoxetine (15mg/kg in the drinking water, for 2 weeks) facilitated extinction of the freezing response in the contextual fear conditioning paradigm, but this effect was lost in mice carrying the TRKB.Y433F mutation (Fig. 4D).

Finally, as observed before, chronic fluoxetine treatment (10mg/kg, in the drinking water for 4 weeks) reactivated critical period-like plasticity in the visual cortex of adult mice [31] (Fig. 4G). A similar induction of ocular dominance plasticity was seen in response to ketamine and R,R-HNK (10mg/kg, ip, three injections in alternate days; Fig. 4G). The effect of fluoxetine on the shift in ocular dominance was lost in TRKB.Y433F heterozygous mice (Fig. 4H), indicating that the plasticity-inducing effects of antidepressants are mediated by their direct binding to TRKB.

Discussion

Here we demonstrate that cholesterol-induced changes in the membrane thickness alter the relative orientation of TRKB dimers, which promotes TRKB surface expression and BDNF signaling. Cholesterol played a permissive role in BDNF-induced TRKB activation, but high cholesterol concentrations limited BDNF signaling. This agrees with previous studies showing that TRKB predominantly resides outside lipid rafts but can transiently signal in these domains [13]. Mutation in the TRKB cholesterol-interaction site limits BDNF signaling, inhibits theta-burst- induced LTP, and prevents antidepressant-induced learning and ocular dominance plasticity. Our findings indicate that TRKB may be the critical target through which astrocyte-derived cholesterol promotes synaptic function and plasticity [16].

BDNF signaling is crucial to the action of essentially all antidepressant drugs, but this effect has been assumed to be indirect, through other molecules such as 5HTT or NMDA receptors. We now show that antidepressants directly bind to the transmembrane region of TRKB dimers with a therapeutically relevant affinity [24,25], favoring translocation of TRKB to the plasma membrane, where it is accessible to BDNF. This binding is shared by typical tricyclic and SSRI antidepressants, as well as by the rapid-acting ketamine and its metabolite R,R-HNK. Mutagenesis demonstrates the critical role of the CARC motif as the binding site for antidepressants to TRKB, and simulation data reveals that antidepressants stabilize TRKB dimers in a BDNF-activatable conformation that is stable in synaptic membranes with high cholesterol concentrations.

The affinity of ketamine to TRKB is comparable to its affinity to NMDA receptors [8], but SSRIs bind to TRKB with a much lower affinity that they bind to the 5HTT. However, micromolar concentrations of SSRIs are reached in the brain during chronic treatment [24,25]. The gradual brain accumulation of typical antidepressants to brain at the concentration needed for TRKB binding might be at least one reason why typical antidepressants take so long to act, while the rapid brain penetration of ketamine and R,R-HNK enables fast action.

The present findings that antidepressants bind to TRKB and thereby prolong BDNF signaling directly link the effects of antidepressants to neuronal plasticity [4]. Juvenile-like plasticity induced by these drugs in the adult brain facilitates beneficial adaptation of neuronal networks that have been abnormally wired during development or by stress [10,11], which may explain the superiority of the antidepressant and psychotherapy combination [32]. Our data suggests a new framework for antidepressant action where the drugs bind to the cholesterol-interaction site of TRKB thereby promoting BDNF-induced plasticity, which is permissive for the activity-dependent network rewiring that underlies the clinical antidepressant response.

Acknowledgements: The authors would like to thank Sulo Kolehmainen and Seija Lågas (Neuroscience Center - UH), Marc Baumann and Rabah Soliymani (Department of Biochemistry and Developmental Biology - UH); and the Biomedicum Imaging Unit (BIU) at the University of Helsinki for technical help and Katja Kaurinkoski for language revision. We also thank Drs. Todd Gould (U. of Maryland) and Craig Thomas (NIH) for kindly supplying the R,R-HNK used in this study, Henri Huttunen (UH) for supplying GLuc-coupled raft-restricted FYN construct; and Yves-Alain Barde, Maija Castrén, Heikki Ruskoaho for their insightful comments to the present manuscript.

Funding: Castrén lab was supported by the ERC grant #322742 - iPLASTICITY; EU Joint Programme - Neurodegenerative Disease Research (JPND) CircProt project #301225 and #643417, Sigrid Jusélius Foundation, Jane and Aatos Erkko Foundation, and the Academy of Finland grants #294710 and #307416. Bramham lab was supported by the EU Joint Programme - Neurodegenerative Disease Research (JPND) CircProt project #30122. Lauri lab was funded by the Academy of Finland grant #297211. Vattulainen group was supported by the Academy of Finland (Center of Excellence) #307415, Sigrid Juselius Foundation, Helsinki Institute of Life Science, and CSC - IT Center for Science (computing resources). Normann and Serchov lab was funded by the German Research Council (#SE 2666/2-1) and the Forschungskommission of the Medical Faculty of the University of Freiburg (#SER1149/17). Saarma lab was funded by Jane and Aatos Erkko Foundation. None of the funders had a role in the data acquisition and analysis, or manuscript preparation.

Authors contributions: PCC, CB, IV and EC designed the experiments; PCC, SMF, CAB, VK and CB performed the biochemical experiments with the assistance of LL and IC. MG, GE, TR and IV performed the molecular modeling and simulation experiments. RM and CAB performed the imaging experiments; CC, HA and AS performed intrinsic optical imaging experiments; FW, SP, and SL performed the electrophysiology experiments. PCC, CRAFD, CC, SV, and TS performed the behavioral studies; PCC and EC wrote the manuscript, with the help of MG, TR, CRB, CN, MS and IV.

Competing interests: EC received lecture fee from Janssen-Cilag. All other authors declare no conflict of interest.

Methods

Protein-protein and ligand docking: For simulations, the secondary structure prediction and modeling of the transmembrane domain of TRKB (residues 427-459) were performed using the FMAP (Folding of Membrane-Associated Peptides) server [33]. The initial models of the TRKB transmembrane (TM) (amino acids 427-459) dimers for atomistic MD simulations were generated using the MPDock application of the Rosetta software suite [34]. The drug-binding pocket was characterized by local docking of the drugs to the TRKB TM dimers using the RosettaScripts interface [35].

Molecular Dynamics simulations. All atomistic simulations were performed using Gromacs 2018 [36] employing the Charmm36(m) force field for the protein [37] and lipids [38], TIP3P water model [39], and a compatible ion parameter set [40]. Drug parameters were generated using the CHARMM General Force Field (CGenFF) program [41]. Lipid membranes were comprised of POPC with a varying concentration of cholesterol (0, 20, 40 mol%). All production simulations were performed in the NpT ensemble at a pressure of 1 bar at three different temperatures (310 K, 333 K, 363 K); key data and conclusions are based on 310 K. All protein-membrane systems were constructed using CHARMM-GUI [42], and all simulation parameters were chosen as suggested.

Free energy calculations. All free energy calculations were performed using the free energy perturbation (FEP) method with Hamiltonian replica exchange. The free energies and their statistical errors were estimated with the Multistate Bennett Acceptance Ratio (MBAR) method using the Alchemical Analysis and the pymbar software [43]. The necessary corrections arising due to the added restraints and the decoupled intra-molecular interactions were applied to obtain the final free energy values.

Analysis. All simulations were repeated through several replicas and the total simulation time covering all simulations was >500 microseconds. All analyses of these data were performed using the tools available in Gromacs 2018 and VMD [44], together with in-house scripts and software. A detailed description of simulation systems and parameters is given in supplement file.

Animals: adult male rats were used for *in vivo* BDNF-induced LTP. Adult male and female mice (12-20 weeks): BDNF haploinsufficient, SERT.ko, TRKB.Y433F.het (detailed description in supplement), with respective wild-type littermates, were used in object-location memory, contextual fear conditioning or ocular dominance plasticity. All animals were kept group housed with free access to food and water, except during the experimental sessions. All protocols were approved by local ethical committees (Finland: ESAVI/10300/04.10.07/2016; Norway: 6159; Germany: G-18-88).

Drugs and reagents: cholesterol, beta-cyclodextrin, pravastatin, fluoxetine, imipramine, ketamine, 2R,6R-HNK (R,R-HNK), 2S,6S-HNK, chlorpromazine, isoproterenol, diphenhydramine, BDNF, and NGF. The amino-biotinylation of fluoxetine, R,R-HNK and imipramine was performed using a commercial kit (EZ-Link NHS-PEG4 Biotinylation Kit, #21455, Thermo Scientific) and the reaction efficiency was evaluated by mass spectrometry. Antibodies: TRKB (R&D, #AF1494); PLC-γ1 (CST, #5690); pTRKB.Y515 (CST, #4619); pTRKB.Y816 (CST, #4168); pY (AbD Serotec, #MCA2472B); actin (Santa Cruz, #sc1615); GFP (Abcam, #ab290, #13970); flotillin-2 (CST, #3436); HRP-conjugated anti-Gt IgG (Invitrogen, #61-1620), anti-Rb IgG (BioRad, #170-5046); HRP-conj streptavidin (Thermo Fisher, #21126).

Cell culture and transfections: HEK293T (used for production of GFP-tagged TRKB), MG87.TRKB cells, Neuroblastoma-2A (N2A), and primary cultures of E18 rat embryos (DIV8 for biochemical analysis and DIV14 for FRAP) were cultivated according to previously described protocols [26,45,46]. The cells were transfected (DIV13 for hippocampal neurons) to express GFP- or Luciferase-tagged TRKB (wt or Y433F or Luciferase-tagged FYN fragment, using lipofectamine 2000 according to manufacturer's instructions (#11668019, Thermo Fisher), or calcium phosphate co-precipitation [47], 24-48h prior to the experimental sessions or sample collection.

Determination of TRKB activation and coupling: the TRKB:pY (pTRKB), TRKB:pTRKB.Y816, TRKB:PLC-γ1 and PLC-γ1:pTRKB.Y816 interactions, and surface TRKB were determined by ELISA [26]. Briefly, white 96-well plates (OptiPlate 96F-HB, Perkin Elmer) were coated with capturing anti-TRKB or anti-PLC-γ1 antibody (1:1000) in carbonate buffer (pH= 9.8) overnight (ON) at 4ºC. Following a blocking step with 2%BSA in TBS-T (2 h, RT), samples were incubated ON at 4ºC. The incubation with antibody against PLC-γ1, pTRKB.Y816 or pY (1:2000, ON, 4ºC) was followed by HRP-conjugated anti-Rb IgG (1:5000, 2h, RT) or HRP-conjugated streptavidin (1:10000, 2h, RT). For surface TRKB assay, the MG87.TRKB cells, cultivated in clear bottom 96-well plates (ViewPlate 96, Perkin Elmer), were washed with ice-cold PBS and fixed with 100µl/well of 4% PFA. After washing with PBS and blocking with PBS containing 5% nonfat dry milk and 5% BSA, the samples were incubated with primary anti-TRKB antibody (R&D Systems, #AF1494, 1:1000 in blocking buffer) ON at 4ºC. Following washing, the samples were incubated with HRP-conjugated anti goat IgG (1:5000 in blocking buffer) for 1h at RT. The cells were washed 4x with 200µl of PBS for 10 min each. Finally, the chemiluminescent signal generated by reaction with ECL was analyzed in a plate reader.
The levels of total and phosphorylated TRKB at Y515 or Y816 in MG87.TRKB cells, challenged with BDNF, were measured by western-blotting [48].
For the analysis of TRKB migration to lipid rafts, the samples from transfected N2A cells to express GFP-tagged TRKB.wt or TRKB.Y433F, challenged with BDNF, were processed to isolate detergent-resistant membrane (DRM) fractions in sucrose gradient [49]. N2A cells were seeded at a density of 2.5 million per plate on 10 cm plates and transfected after 24 hours with either wild-type GFP-tagged full length TRKB or the GFP-tagged Y433F TRKB mutant. 48 hours after plating, cells were washed with ice cold 1x PBS and scraped in extraction buffer (25 mM Tris-HCl pH 8, 150 mM NaCl, 5 mM EDTA) with the addition of 0.5% v/v Lubrol (Serva) and a cocktail of protease and phosphatase inhibitors (Sigma). Cellular membranes were mechanically broken by passing the cell suspension through a 23G needle five times. Protein concentration was measured for each sample and equal amounts of proteins were transferred to Eppendorf tubes and mixed with sucrose in extraction buffer to a final concentration of 72% . The samples were then transferred to the bottom of Beckman 2.2 ml ultracentrifuge tubes and carefully covered with equal volumes of 35% sucrose and 5% sucrose in extraction buffer.
The samples were centrifuged at 52000 x g for 18 hours at +4°C with a TLS-55 rotor in a Beckman Coulter XP Optima ultracentrifuge. Finally, 12 fractions per sample, collected from the top of the tube, were transferred to clean tubes, sonicated for 10 minutes in 0.25% SDS and prepared for western blotting, where the levels of GFP-tagged TRKB and flotillin-2 were analyzed.

Protein complementation assay: two complementary fragments of the luciferase reporter protein were fused to the intracellular C-terminus domain of TRKB.wt or mutant TRKB.Y433F to produce the PCA pairs GLuc1C-TRKB.wt/GLuc2C-TRKB.wt and GLuc1C-TRKB.Y433F/GLuc2C-TRKB.Y433F. Alternatively, the GLuc1C-TRKB.wt/GLuc2C-FYN or GLuc1C-TRKB.Y433F/GLuc2C-FYN pairs were used. The GLuc2C-FYN construct expresses a lipid-raft restricted fragment of Src-family kinase FYN. The GLuc tag was linked via a GS linker that allows the physiological dynamics of proteins without interferences from the presence of the tag. N2A cells, in 10% (v/v) poly-L-Lysine coated 96 wells (10,000 cells/well) were transfected with the construct pairs above. Cells were treated 48h post-transfection with BDNF (10ng/ml/10min), and luminescence measured as a direct indication of TRKB homodimerization or TRKB:LR-FYN with a plate reader (Varioskan Flash, Thermo Scientific, average of 5 measurements, 0.1 second each) immediately after the injection of the coelenterazine substrate (Nanolight Technology).

Cell viability: the assay was performed using CellTiterGlo (#G7571; Promega) according to manufacturer's instructions. Briefly, equal amounts of medium and the mixture of regents A and B were added to the E18 cortical cells (DIV8) and incubated for 40min in clear bottom 96-well plates. . The cells were previously treated with BDNF (10ng/ml/5d), cholesterol (20µM/5d) or combo and pravastatin (2µM/5d). The luminescence was analyzed in a plate reader.

Drug binding assay: the drug/BDNF interaction with TRKB was determined by ELISA, based on similar assays in literature [50]. TRKB.wt or TRKB.Y433F were expressed in HEK293T cells, and immunoprecipitated in 96-well plates. Increasing doses of

biotinylated drugs fluoxetine or R,R-HNK (0.1-100µM), tritiated imipramine (0.01-30µM) or biotinylated BDNF (0.1-100ng/ml) were added after blocking with 2% BSA in PBS for 1h and the signal developed by incubation with HRP-conjugated streptavidin followed by ECL. For the competitive assay, increased doses of non-biotinylated drugs (0.1-10µM) or BDNF (10-100ng/ml) were mixed with 1µM of biotinylated fluoxetine for 1h, and the signal from HRP-conjugated streptavidin developed as described above. Microscale Thermophoresis - MST - was performed according to literature [23]. Briefly, the changes in fluorescence following temperature gradient emitted by GFP-TRKB, incubated with fluoxetine (0-100µM) were conducted in premium coated capillaries using LED source with 470nm and 50% infrared-laser power.

FRAP: hippocampal cells from E18 rat embryos (DIV14) were transfected to express GFP-TRKB.wt or GFP-TRKB.Y433F. Upon identification of GFP-positive cells, the cells were treated with fluoxetine, ketamine or BDNF for 15min; the whole spine head or the neurite shaft was bleached with high laser power [51] and the latency for fluorescence recovery was quantified.

TIRF/dSTORM: MG87.TRKB cells were transfected to overexpress GFP-TRKB.wt or GFP-TRKB.Y433F, challenged with BDNFor fluoxetine for 15min and fixed to immunostaining for GFP. The area of GFP-tagged TRKB cell surface clusters was determined by total internal reflection fluorescence microscopy (TIRF) coupled with direct stochastic optical reconstruction microscopy (dSTORM).

Immunostaining and Sholl analysis: cortical cells (E18 rat embryo, DIV8) were treated with BDNF (10ng/ml/3d) and pravastatin (1µM/3d), fixed and labeled for actin. The number of intersections from the cell body was counted using FIJI plug-in [52].

Electrophysiology (details in supplement): in vivo and ex vivo
In vivo BDNF-induced LTP was performed according to literature [27]. Briefly, pravastatin was administered in drinking water at a dose of 10mg/kg/day for 15-17 days calculated on the basis of daily body weight. Rats were anesthetized with an intraperitoneal injection of urethane 1.5 g/kg body weight, positioned in a stereotaxic frame, and Teflon-coated tungsten wire recording electrode was placed in the dentate hilus. The tip of the infusion cannula was located in the deep stratum lacunosum-moleculare of field CA1, 800µm above the hilar recording site and 300-400µm above the medial perforant synapse. After baseline recording for 20 min, infusion of 2µl of 1 µg/µl BDNF over 30 min at a rate of 0.067µl/min. Evoked responses were recorded for 120 min after infusion.
Ex vivo activity-induced LTP: TBS and tetanus stimulus was performed according to literature [53]. Briefly, mice were deeply anaesthetized with isoflurane, the brains were dissected and horizontal 350 micrometers brain slices of the hippocampus were cut on a vibratome. Field excitatory postsynaptic currents (EPSPs) were recorded at the stratum radiatum of the CA1 region. Electric stimulation was delivered by a bipolar concentric stimulation electrode placed at the Schaffer collateral. After obtaining a 15 min stable baseline theta burst stimulation (TBS: 10 bursts of four pulses at 100 Hz, with an interburst interval of 200 msec) or tetanic stimulation (200ms pulse interval; 100 pulses; 0.1ms pulse duration) was delivered and field potentials were recorded for 45 min.

Ocular dominance plasticity assay (details in supplement):
The shift in ocular dominance induced by drug treatment was performed according to literature [31]. Briefly, animals were anesthetized via i.p. injection with a mixture containing: 0.05 mg/kg fentanyl; 5 mg/kg midazolam; 0.5 mg/kg medetomidine; diluted in saline and fixed in the stereotaxic frame. After cleaning and polishing, a thin layer of cyanoacrylate glue was applied to the surface of the skull, in order to make it transparent. The next day, the acryl layer was polished over the area of interest. A metal head holder was first glued on the skull, carefully keeping the area of interest at the center of the holder, and then fixed with a mixture of cyanoacrylate glue and dental cement. Finally, transparent nail polisher (#72180, Electron Microscopy Sciences) was applied inside the metal holder above the area of interest. Monocular deprivation was carried on the left eye, the eyelashes were cut and the eye sutured shut with 3 mattress sutures. The monocular deprivation lasted 8 days and the animals were checked daily and resutured if needed to prevent reopening of the eyes. Two sessions of imaging were performed: one before the beginning of the treatment with fluoxetine, ketamine or R,R-HNK (IOS I) and one on the 8th day after monocular deprivation (IOS II). For imaging, animals were kept on a heating pad located in front of and within 25 cm from the stimulus monitor. The visual stimulus was a 2° wide horizontal bar moving upwards with a temporal frequency of 0.125 Hz and a spatial frequency of 1/80 degree, displayed in the central part of a high refresh rate monitor (-15 to 5 degrees azimuth, relative to the animal visual field) in order to preferentially stimulate the binocular part of the visual field. The continuous-periodic stimulation was synchronized with a continuous frame acquisition, frames were collected independently for each eye. After obtaining cortical maps for both contralateral (C) and ipsilateral (I) eyes and computing Ocular Dominance score as (C−I)/(C+I), finally, the Optical Dominance Index (ODI) was calculated as the mean of the OD score for all responsive pixels. The ODI values are comprised in an interval going from -1 to +1: positive values indicate a contralateral bias, negative ones indicate ipsilateral bias and ODI values of 0 indicate that ipsilateral and contralateral eyes are equally strong.

Behavioral analysis:
Object-location memory (OLM): this test was performed in a square arena (28cm side) with opaque walls containing cues (black stripes or spots). The mice were placed for 3 consecutive days (15min per session) in the arena with two identical objects (table tennis balls glued to caps of 50ml Falcon tubes) in the same position throughout the sessions (pretest). Following the drug administration (starting immediately after the last pretest session). At the test session one of the objects is moved to a different position and the number of visits (counted as sniffing or interacting with the object) to the old (A) or newly located (A') object was determined by an observer blind to the conditions [54,55].
Contextual fear conditioning: this test was modified from previous studies [11]. Briefly, the mice were conditioned to 5 scrambled foot shocks (0.6mA/2s) during the 8 min session (arena: 23×23×35cm) under constant illumination (100 lux). The treatment with fluoxetine started immediately after the conditioning session throughout the last extinction trial. During the extinction trials, the animals were exposed to the same context where the shocks were delivered and the time spent in freezing during the 8 min session was automatically determined by the software (TSE Systems, Germany).

Forced swimming test - FST: animals were submitted to a 6min session of FST in 5-liter glass beaker cylinders (19cm diameter, with 20cm water column 25±1°C) [56]. Fluoxetine was administered for 3weeks (15mg/kg, in the drinking water), and ketamine was injected 2h (ip) prior to the FST. The immobility was assessed in the last 4min of the session, and the water was changed between each test. After swimming, animals were kept in a warm cage until dried, then returned to their home cages. Test was videotaped and analyzed by a trained observer blind to treatment.

Statistics: Student's t test (two-tailed), one- or two-way ANOVA were used, followed by Fisher's LSD *post hoc* test. *F* and *p* values are indicated in Table S2.

References

1. Park, H. & Poo, M.-M. Neurotrophin regulation of neural circuit development and function. *Nat. Rev. Neurosci.* **14**, 7–23 (2013).
2. Duman, R. S. & Monteggia, L. M. A neurotrophic model for stress-related mood disorders. *Biol. Psychiatry* **59**, 1116–1127 (2006).
3. Autry, A. E. & Monteggia, L. M. Brain-derived neurotrophic factor and neuropsychiatric disorders. *Pharmacol. Rev.* **64**, 238–258 (2012).
4. Castrén, E. & Antila, H. Neuronal plasticity and neurotrophic factors in drug responses. *Mol. Psychiatry* (2017) doi:10.1038/mp.2017.61.
5. Belmaker, R. H. & Agam, G. Major depressive disorder. *N. Engl. J. Med.* **358**, 55–68 (2008).
6. Abdallah, C. G., Sanacora, G., Duman, R. S. & Krystal, J. H. Ketamine and rapid-acting antidepressants: a window into a new neurobiology for mood disorder therapeutics. *Annu. Rev. Med.* **66**, 509–523 (2015).
7. Zanos, P. *et al.* NMDAR inhibition-independent antidepressant actions of ketamine metabolites. *Nature* **533**, 481–486 (2016).
8. Zanos, P. *et al.* Ketamine and Ketamine Metabolite Pharmacology: Insights into Therapeutic Mechanisms. *Pharmacol. Rev.* **70**, 621–660 (2018).
9. Saarelainen, T. *et al.* Activation of the TrkB neurotrophin receptor is induced by antidepressant drugs and is required for antidepressant-induced behavioral effects. *J. Neurosci.* **23**, 349–357 (2003).
10. Maya Vetencourt, J. F. *et al.* The antidepressant fluoxetine restores plasticity in the adult visual cortex. *Science* **320**, 385–388 (2008).
11. Karpova, N. N. *et al.* Fear erasure in mice requires synergy between antidepressant drugs and extinction training. *Science* **334**, 1731–1734 (2011).
12. Zonta, B. & Minichiello, L. Synaptic membrane rafts: traffic lights for local neurotrophin signaling? *Front. Synaptic Neurosci.* **5**, (2013).
13. Suzuki, S. *et al.* Brain-Derived Neurotrophic Factor Regulates Cholesterol Metabolism for Synapse Development. *Journal of Neuroscience* **27**, 6417–6427 (2007).
14. Suzuki, S. *et al.* BDNF-induced recruitment of TrkB receptor into neuronal lipid rafts: roles in synaptic modulation. *J. Cell Biol.* **167**, 1205–1215 (2004).
15. Martin, M. G. *et al.* Constitutive hippocampal cholesterol loss underlies poor cognition in old rodents. *EMBO Mol. Med.* **6**, 902–917 (2014).
16. Pfrieger, F. W. & Ungerer, N. Cholesterol metabolism in neurons and astrocytes. *Prog. Lipid Res.* **50**, 357–371 (2011).
17. Tulodziecka, K. *et al.* Remodeling of the postsynaptic plasma membrane during neural development. *Mol. Biol. Cell* **27**, 3480–3489 (2016).
18. Di Lieto, A. *et al.* The responsiveness of TrkB to BDNF and antidepressant drugs is differentially regulated during mouse development. *PLoS One* **7**, e32869 (2012).
19. Wray, N. H., Schappi, J. M., Singh, H., Senese, N. B. & Rasenick, M. M. NMDAR-independent, cAMP-dependent antidepressant actions of ketamine. *Mol. Psychiatry* (2018) doi:10.1038/s41380-018-0083-8.
20. Fantini, J., Epand, R. M. & Barrantes, F. J. Cholesterol-Recognition Motifs in Membrane Proteins. *Adv. Exp. Med. Biol.* **1135**, 3–25 (2019).
21. Fantini, J. & Barrantes, F. J. How cholesterol interacts with membrane proteins: an exploration of cholesterol-binding sites including CRAC, CARC, and tilted domains. *Front. Physiol.* **4**, (2013).
22. Arkhipov, A. *et al.* Architecture and membrane interactions of the EGF receptor. *Cell* **152**, 557–569 (2013).
23. Jerabek-Willemsen, M. *et al.* MicroScale Thermophoresis: Interaction analysis and beyond. *J. Mol. Struct.* **1077**, 101–113 (2014).
24. Bolo, N. R. *et al.* Brain pharmacokinetics and tissue distribution in vivo of fluvoxamine and fluoxetine by fluorine magnetic resonance spectroscopy. *Neuropsychopharmacology* **23**, 428–438 (2000).
25. Karson, C. N. *et al.* Human brain fluoxetine concentrations. *J. Neuropsychiatry Clin. Neurosci.* **5**, 322–329 (1993).
26. Fred, S. M. *et al.* Pharmacologically diverse antidepressants facilitate TRKB receptor activation by disrupting its interaction with the endocytic adaptor complex AP-2. *J. Biol. Chem.* (2019) doi:10.1074/jbc.RA119.008837.
27. Panja, D. & Bramham, C. R. BDNF mechanisms in late LTP formation: A synthesis and breakdown. *Neuropharmacology* **76 Pt C**, 664–676 (2014).
28. Minichiello, L. *et al.* Mechanism of TrkB-mediated hippocampal long-term potentiation. *Neuron* **36**, 121–137 (2002).
29. Normann, C. *et al.* Antidepressants Rescue Stress-Induced Disruption of Synaptic Plasticity via Serotonin Transporter-Independent Inhibition of L-Type Calcium Channels. *Biol. Psychiatry* **84**, 55–64 (2018).
30. Nackenoff, A. G., Moussa-Tooks, A. B., McMeekin, A. M., Veenstra-VanderWeele, J. & Blakely, R. D. Essential Contributions of Serotonin Transporter Inhibition to the Acute and Chronic Actions of Fluoxetine and Citalopram in the SERT Met172 Mouse. *Neuropsychopharmacology* **41**, 1733–1741 (2016).
31. Steinzeig, A., Molotkov, D. & Castrén, E. Chronic imaging through 'transparent skull' in mice. *PLoS One* **12**, e0181788 (2017).
32. Pampallona, S., Bollini, P., Tibaldi, G., Kupelnick, B. & Munizza, C. Combined pharmacotherapy and psychological treatment for depression: a systematic review. *Arch. Gen. Psychiatry* **61**, 714–719 (2004).
33. Lomize, A. L., Hage, J. M. & Pogozheva, I. D. Membranome 2.0: database for proteome-wide profiling of bitopic proteins and their dimers. *Bioinformatics* **34**, 1061–1062 (2018).
34. Alford, R. F. *et al.* An Integrated Framework Advancing Membrane Protein Modeling and Design. *PLoS Comput. Biol.* **11**, e1004398 (2015).
35. Fleishman, S. J. *et al.* RosettaScripts: a scripting language interface to the Rosetta macromolecular modeling suite. *PLoS One*

6, e20161 (2011).
36. Abraham, M. J. *et al.* GROMACS: High performance molecular simulations through multi-level parallelism from laptops to supercomputers. *SoftwareX* **1-2**, 19–25 (2015).
37. Huang, J. *et al.* CHARMM36m: an improved force field for folded and intrinsically disordered proteins. *Nat. Methods* **14**, 71–73 (2017).
38. Klauda, J. B. *et al.* Update of the CHARMM all-atom additive force field for lipids: validation on six lipid types. *J. Phys. Chem. B* **114**, 7830–7843 (2010).
39. Jorgensen, W. L., Chandrasekhar, J., Madura, J. D., Impey, R. W. & Klein, M. L. Comparison of simple potential functions for simulating liquid water. *J. Chem. Phys.* **79**, 926–935 (1983).
40. Beglov, D. & Roux, B. Finite representation of an infinite bulk system: Solvent boundary potential for computer simulations. *J. Chem. Phys.* **100**, 9050–9063 (1994).
41. Vanommeslaeghe, K. *et al.* CHARMM general force field: A force field for drug-like molecules compatible with the CHARMM all-atom additive biological force fields. *J. Comput. Chem.* **31**, 671–690 (2009).
42. Jo, S., Kim, T., Iyer, V. G. & Im, W. CHARMM-GUI: a web-based graphical user interface for CHARMM. *J. Comput. Chem.* **29**, 1859–1865 (2008).
43. Klimovich, P. V., Shirts, M. R. & Mobley, D. L. Guidelines for the analysis of free energy calculations. *J. Comput. Aided Mol. Des.* **29**, 397–411 (2015).
44. Humphrey, W., Dalke, A. & Schulten, K. VMD: visual molecular dynamics. *J. Mol. Graph.* **14**, 33–8, 27–8 (1996).
45. Sahu, M. P., Nikkilä, O., Lågas, S., Kolehmainen, S. & Castrén, E. Culturing primary neurons from rat hippocampus and cortex. *Neuronal Signaling* **3**, NS20180207 (2019).
46. Antila, H. *et al.* Utilization of in situ ELISA method for examining Trk receptor phosphorylation in cultured cells. *J. Neurosci. Methods* **222**, 142–146 (2014).
47. Xia, Z., Dudek, H., Miranti, C. K. & Greenberg, M. E. Calcium influx via the NMDA receptor induces immediate early gene transcription by a MAP kinase/ERK-dependent mechanism. *J. Neurosci.* **16**, 5425–5436 (1996).
48. Rantamäki, T. *et al.* Pharmacologically diverse antidepressants rapidly activate brain-derived neurotrophic factor receptor TrkB and induce phospholipase-Cgamma signaling pathways in mouse brain. *Neuropsychopharmacology* **32**, 2152–2162 (2007).
49. McGuinn, K. P. & Mahoney, M. G. Lipid rafts and detergent-resistant membranes in epithelial keratinocytes. *Methods Mol. Biol.* **1195**, 133–144 (2014).
50. Das, I. *et al.* Preventing proteostasis diseases by selective inhibition of a phosphatase regulatory subunit. *Science* **348**, 239–242 (2015).
51. Koskinen, M., Bertling, E. & Hotulainen, P. Methods to measure actin treadmilling rate in dendritic spines. *Methods Enzymol.* **505**, 47–58 (2012).
52. Schindelin, J. *et al.* Fiji: an open-source platform for biological-image analysis. *Nat. Methods* **9**, 676–682 (2012).
53. Popova, D., Castrén, E. & Taira, T. Chronic fluoxetine administration enhances synaptic plasticity and increases functional dynamics in hippocampal CA3-CA1 synapses. *Neuropharmacology* **126**, 250–256 (2017).
54. Dere, E., Huston, J. P. & De Souza Silva, M. A. The pharmacology, neuroanatomy and neurogenetics of one-trial object recognition in rodents. *Neurosci. Biobehav. Rev.* **31**, 673–704 (2007).
55. Ampuero, E. *et al.* Repetitive fluoxetine treatment affects long-term memories but not learning. *Behav. Brain Res.* **247**, 92–100 (2013).
56. Diniz, C. R. A. F. *et al.* Antidepressant-like effect of losartan involves TRKB transactivation from angiotensin receptor type 2 (AGTR2) and recruitment of FYN. *Neuropharmacology* **135**, 163–171 (2018).

Figures and legends

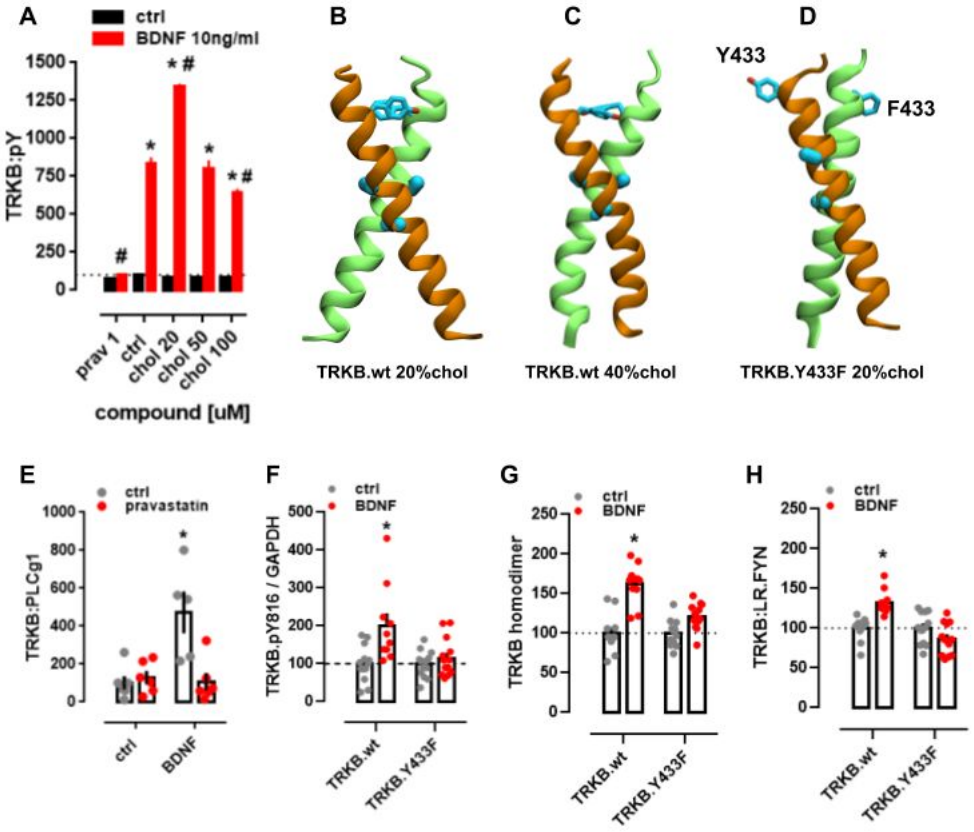

Figure 1. Identification of cholesterol-interacting motif (CARC) in TRKB. (A) Dual effect of cholesterol in BDNF-induced activation of TRKB (n=6/group). (B-C) Structures for wild-type TRKB at cholesterol concentrations of 20 mol% and 40 mol%, and (D) for the TRKB.wt and TRKB.Y433F heterodimer at 20 mol% (systems 1-4, Table S1, Fig. S2 for distance and α values between C-termini). (E) BDNF-induced increase in TRKB:PLC-γ1 is prevented by previous treatment with pravastatin (n=6, 6, 5, 6). (F) BDNF-induced phosphorylation of TRKB at Y816 is prevented in the TRKB.Y433F mutant (n=13, 14, 10, 14). (G) The BDNF-induced dimerization of TRKB is also compromised by the Y433F mutation (n=11, 12, 11, 12), (H) as well as the BDNF-induced increase in TRKB interaction with FYN fragment in lipid raft (n=12/group).

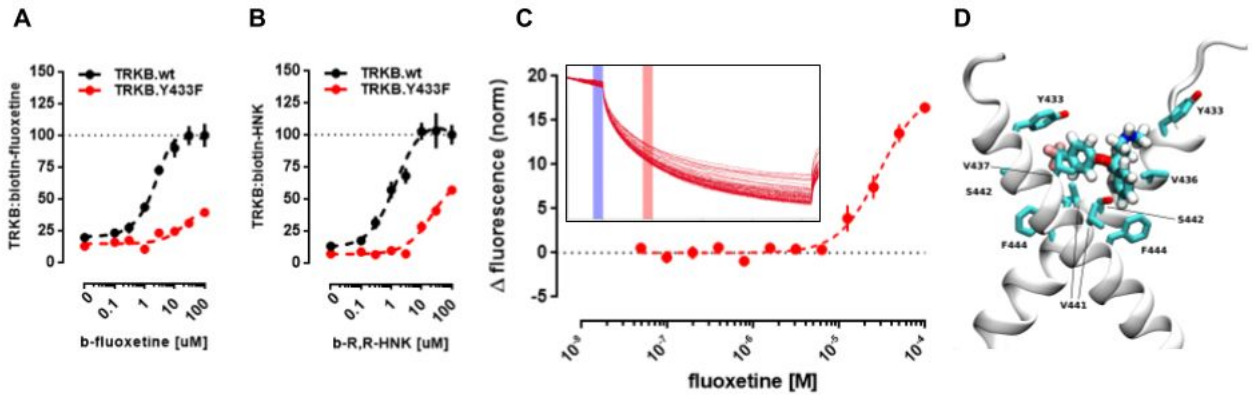

Figure 2. Binding of antidepressants to TRKB. Binding of biotinylated (A) fluoxetine and (B) R,R-HNK to precipitated TRKB.wt or TRKB.Y433F (fluoxetine: TRKB.wt n=14, 14, 9, 12, 6, 12, 9, 14; TRKB.Y433F n=12, 12, 9, 9, 6, 10, 9, 12; R,R-HNK: TRKB.wt n=14, 14, 6, 14, 6, 14, 6, 14; TRKB.Y433F n=14, 14, 6, 14, 6, 14, 6, 14). Data expressed as percentage of saturated binding (100µM). (C) Fluoxetine interacts with GFP-tagged TRKB as observed by microscale thermophoresis (n=4/group). Experimental traces depicted in the insert, vertical bars: blue= fluorescence cold, red= fluorescence hot. (D) Representation of fluoxetine binding to the pocket formed by dimerization of the TRKB transmembrane domains.

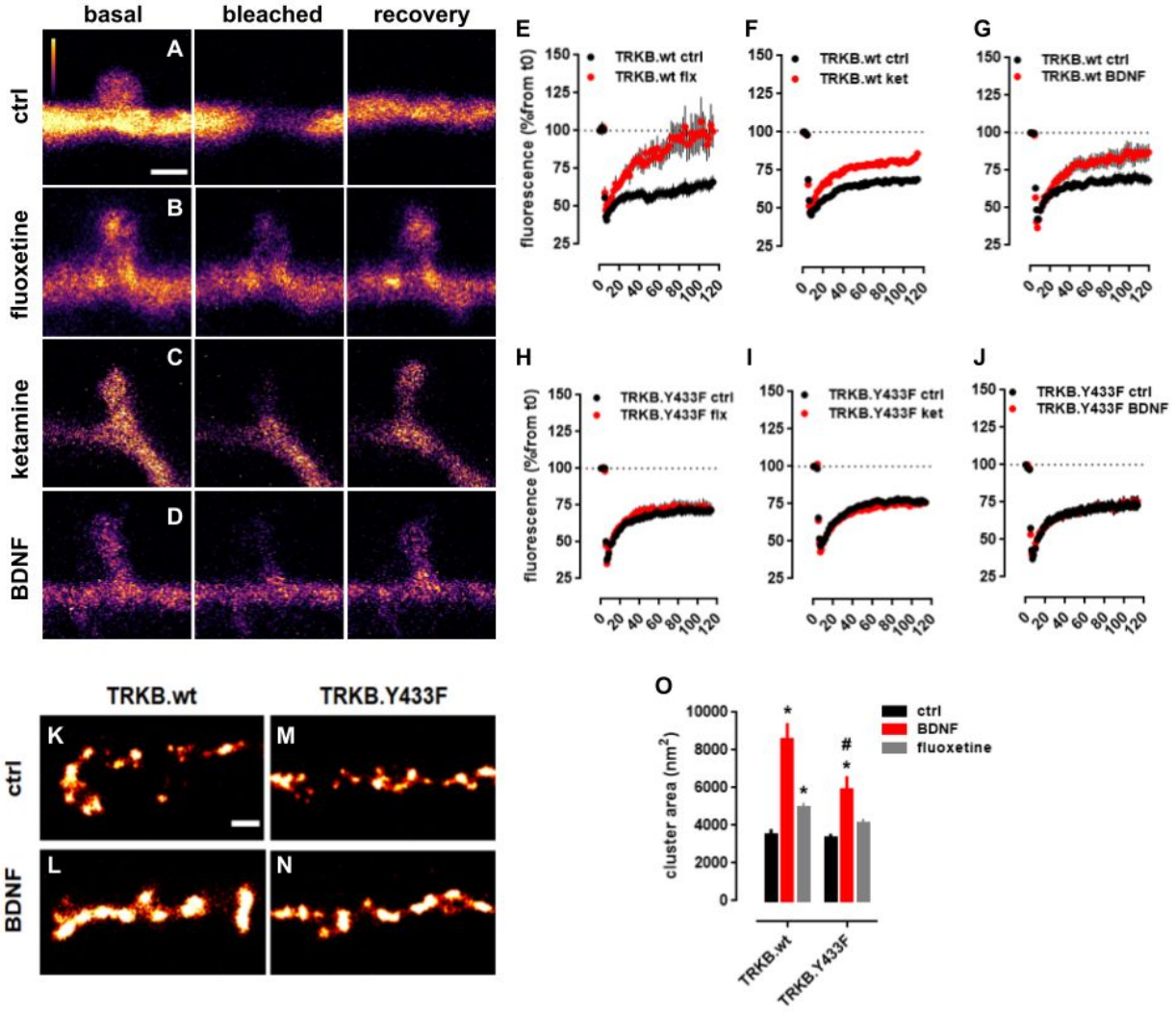

Figure 3. Effects of BDNF and antidepressants on TRKB trafficking. Representative images of the spine and shaft fluorescence in (A) control, (B) fluoxetine, (C) ketamine or (D) BDNF treated rat hippocampal neurons (E18; DIV14) transfected with GFP-TRKB before (basal), immediately (bleached) and 2 min (recovery) after photobleaching (for analysis of neurite shaft recovery see Fig. S6A). Scale bar: 1000nm. (E, H): Fluoxetine (1µM/15min, TRKB.wt n=22, 9; TRKB.Y433F n=42, 28), (F,I) ketamine (10 µM/15min,TRKB.wt n=18, 15; TRKB.Y433F n=22, 20) and (G,J) BDNF (10ng/ml/15min, TRKB.wt n=27, 17; TRKB.Y433F n=39, 27) trigger the recovery of GFP-TRKB in dendritic spines but this is prevented in GFP-TRKB.Y433F expressing neurons; data expressed as mean±SEM of percentage from t=0. (K-N) Representative images of the BDNF-induced clusters of GFP-TRKB in the surface of MG87.TRKB cells. Scale bar: 250nm. (O) BDNF (10 ng/ml/15 min) and fluoxetine (10 µM/15min, TRKB.wt n= 444, 365 593; TRKB.Y433F n= 542, 232, 547) enhance the formation of clusters of GFP-TRKB on the surface of MG87.TRKB cells but not in the GFP-TRKB.Y433F expressing cells. *p<0.05 from respective control (vehicle-treated) groups; #p<0.05 from BDNF- or fluoxetine-treated wt group (Fisher's LSD), n=232-542 clusters from 10 cells/group, and 10 regions of interest (ROI) per image, mean±SEM of cluster area (nm^2).

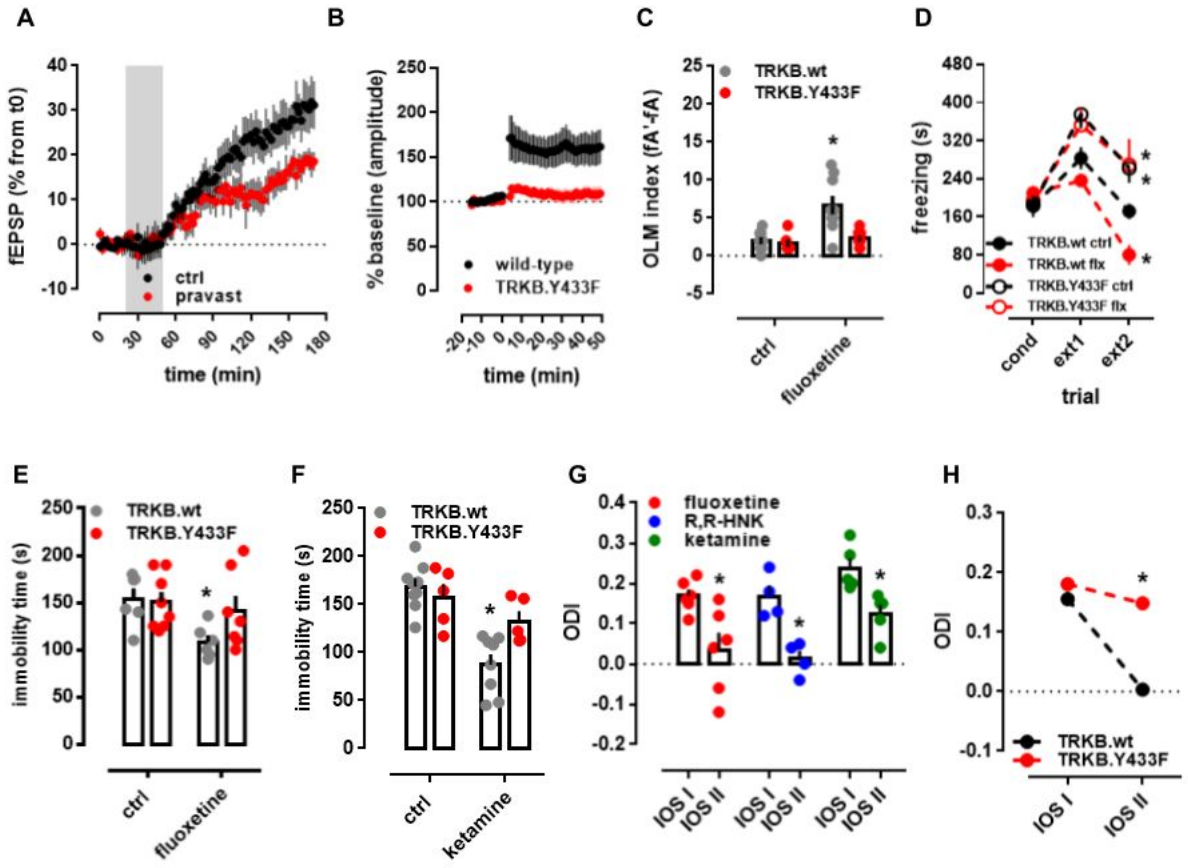

Figure 4. Role of TRKB CARC in drug induced plasticity. (A) BDNF-induced LTP in rat dentate gyrus is attenuated by pravastatin administration (ctrl n=8, pravastatin n=9). (B) Theta-burst induced LTP in the CA3-CA1 synapses of hippocampal slices from wild-type mice, but not in slices from Y433F mutant mice; mean±SEM from baseline [in A t=0; in B t= -20min]. (C) Fluoxetine improved object location memory (OLM) in wild-type mice, but this effect was absent in the TRKB.Y433F mice (n=8, 9, 6, 8). (D) Fluoxetine facilitated the extinction of contextual conditioned fear, and this response is blocked in mice carrying the TRKB.Y433F mutation (n=5, 5, 5, 6). *p<0.05 from ctrl/ctrl or ctrl/wt group in the same session (Fisher's LSD), mean±SEM of total freezing time in the 8 min session. (E) fluoxetine (n=6, 6, 8, 7) and (F) ketamine (n=9, 8, 5, 5) reduce immobility in the forced swim test in TRKB.WT mice, but are ineffective in TRKB.Y433F mutants. *p<0.05 from ctrl/wt group. (G) Fluoxetine (0.08 mg/l p.o. for 28 days, n=6), R,R-HNK (10mg/kg every second day for 6 days, n=4) and ketamine (10mg/kg every second day for 6 days, n=4) permitted a shift in ocular dominance in adult mice during 7 days of monocular deprivation. *p<0.05 between intrinsic signal imaging (IOS) sessions before and after monocular deprivation (Fisher's LSD), mean±SEM of ocular dominance index (ODI). (H) Fluoxetine (10mg/kg/day for 28 days) fails to permit a shift in ocular dominance in TRKB.Y433F mice (n=6, 7). *p<0.05 from vehicle-treated group in the same session (Fisher's LSD),mean±SEM.